Journal of Wind Engineering and Industrial Aerodynamics, 25 (1986) 49—74
Elsevier Science Publishers B.V., Amsterdam — Printed in The Netherlands

PERTURBATION ANALYSIS AND MEASUREMENTS OF BUILDING WAKES IN A STABLY STRATIFIED TURBULENT BOUNDARY LAYER

K.M. KOTHARI*, J.A. PETERKA and R.N. MERONEY

Fluid Mechanics and Wind Engineering Program, Department of Civil Engineering, Colorado State University, Colorado (U.S.A.)

(Received November 1, 1984; accepted in revised form April 22, 1986)

Summary

Velocity and temperature wakes behind obstacles deeply submerged in a stably stratified turbulent boundary layer with one face perpendicular to the flow direction were investigated using wind-tunnel tests and mathematical analysis. For stably stratified approach flow, the effects of a building wake characterized by momentum deficit are to decrease mean velocity and mean temperature but to increase turbulence intensity and temperature fluctuation intensity. On the other hand, along the centerline of a building wake, mean velocity and mean temperature increase and turbulent intensity and temperature-fluctuation intensity decrease in the presence of longitudinal horseshoe vortices. A perturbation technique for determining the temperature distribution in the wake of an isolated building was developed using momentum and vortex wake arguments. Hunt's theory for velocity distribution in a "momentum" and "vortex" wake and a modified method developed by the writers for temperature distributions agreed with measurements of mean velocity and temperature distributions.

1. Introduction

The perturbation introduced into the atmospheric surface layer by man-made structures may uniquely influence man's comfort, safety, and efficiency. Changes in turbulence structure and flow streamlines downwind of a large building are contained within a "wake" influence region. Diffusion of material released in the wake of a building is strongly altered, particularly if the pollutant is released within the separated region in the lee of a building. Local pressure (structural) loading may increase or decrease due to nearby structures, and may depend on the relative position of approaching wind, the building shapes, and separation distances between the structures. Pedestrian comfort near a building is frequently influenced by the building wake characteristics. Wind structure on airport runways may be affected by nearby building wakes.

Visualization of fluid particle motion and measurements of wake structure in the laboratory and behind prototype structures has led to the

*Present address: Project Manager, Gas Research Institute, 8600 W. Bryn Mawr Avenue, Chicago, IL 60601, U.S.A.

0167-6105/86/$03.50

development of flow models which predict the building wake behavior in a neutral turbulent boundary layer. The object of this paper is to analyze the effects on the building wake of thermal stability in the approach flow. A program of laboratory measurements was made behind simple building structures immersed in a stably stratified shear flow. A perturbation model is presented which predicts the mean temperature distribution in the wake of a building.

2. Building wakes

2.1. Field measurements

High cost, limited data acquisition, and the nonstationary character of the atmosphere have severely limited the availability of field measurements of building wakes. Since this paper deals with three-dimensional wake structure, the literature related to two-dimensional fence wakes is not included.

Prototype measurements have been reported by Colmer [1] for the wake of a hanger at the Royal Aircraft Establishment at Bedford, and by Frost and Shahabi [2] for rectangular buildings at the NASA Marshall Space Flight Center in Huntsville, Alabama. In Colmer's experiment, three instrumented towers were located along the principal wind direction centerline, with one tower off the centerline. Upwind flow conditions were measured by a tower 18 building heights upstream of the hanger. The mean speed in the wake was found to be smaller and the turbulence intensity was higher than in the approach flow. Colmer also reported that the mean velocity wake disappeared by 15 building heights downstream. However, the turbulent intensity wake was still present 23 heights downstream of the hanger.

Frost and Shahabi [2] reported measurements of mean longitudinal velocity, vertical velocity, wind direction, and auto-correlations and spectra of longitudinal velocity fluctuations in the wake of a small building 2.4 m deep, 3.2 m high, and 7.95 m long, and in the wake of a longer building 2.4 m deep, 3.2 m high, and 26.8 m long. The mean velocity defect, the difference between mean velocity in the approach flow and in the wake at the same height, decayed with distance at a rate proportional to $x^{-1.5}$, agreeing with wind-tunnel measurements of Woo et al. [3] and the theory of Hunt and Smith [4].

2.2. Laboratory measurements

The first intensive laboratory measurements of building wakes were conducted by Counihan [5]. He measured mean velocity, fluctuating velocity, and spectra in the wakes of a two-dimensional fence and a cube placed in a simulated turbulent boundary layer with a mean 0.15 power-law velocity profile. Counihan found that the mean velocity defect decay rate for the two-dimensional block was smaller than that of the three-dimensional cube. The scales of turbulence detected were smaller in the wake region than in the boundary-layer approach flow. Castro and Robins [6] per-

formed similar experiments in a rougher boundary layer in the near wake of cubical buildings.

Lemberg [7] obtained wake data behind obstacles placed in a turbulent boundary layer. Measurements included longitudinal mean and rms velocities, and the drag force on the obstacle. The velocity defect was found to decay as $x^{-1.58}$; however, the decay of turbulence intensity excess, the difference between turbulence intensity in the wake of a building and in the approach flow at the same height, was much slower, and it varied from $x^{-0.11}$ to $x^{-0.30}$. He also observed the characteristic horseshoe vortices wrapped around the building during a flow visualization study in a water channel, but he did not attempt to determine their effect on the wake envelope.

Other wake measurements were reported by Hansen et al. [8], Woo et al. [3], Peterka and Cermak [9], and Hansen and Cermak [10]. They examined the effect of approach flow direction on the wake structure. For certain building shapes, the wake extends about four times farther when the building is placed at 45 degrees to the approach flow than when one face is normal to the approach flow.

Hunt et al. [11] discussed kinematical aspects of the flow around free or surface-mounted obstacles. They deduced the mean surface stress streamlines from surface oil-flow patterns. The mean flow streamlines were sketched using derived relations for shear-stress singular points. They concluded that closed streamline surfaces do not exist in the separated flow around surface-mounted obstacles.

2.3. Theoretical methods

A theoretical foundation for building wake flow structure has been pioneered by Hunt and Smith [4], who proposed a theory to calculate mean velocity in the wake of two- and three-dimensional bluff bodies immersed in a thick turbulent boundary layer. This momentum-wake theory is based on the assumptions that an obstacle causes small perturbations to the turbulent boundary layer, that the ratio of the obstacle height to the boundary-layer height is small, that the velocity profile power-law exponent is small, and that the mixing may be represented by a constant eddy viscosity. This theory is only valid for the far wake region ($x/H > 5$), because the separated region behind the building cannot be considered to be a small perturbation on the approach flow. The two-dimensional theory was described in detail by Counihan et al. [12]. Hunt's [13] three-dimensional momentum-wake theory predicts (see Fig. 1 for coordinates and wake schematic):

$$\frac{u(x, y, z)}{\overline{U}(H)} = k_1 F_1(z'', y'')/[(x - a)/H]^{(3+n)/(2+n)} \tag{2.1}$$

where:

$u(x, y, z)$ = velocity defect,

$\overline{U}(H)$ = velocity at building height H in the undisturbed flow,

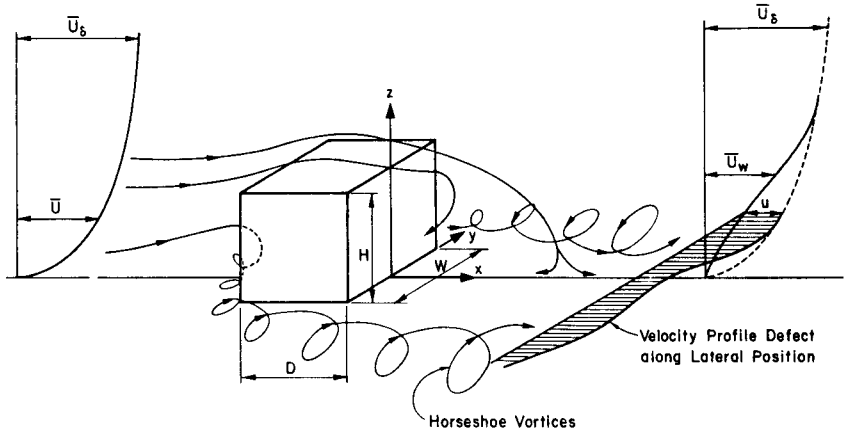

Fig. 1. Experimental configuration, definition of symbols and flow around a rectangular block.

a = virtual origin of the wake to be determined from experiment,

n = boundary layer velocity profile power-law exponent,

k_1 = $0.21\, C_{Fx}\,(W/H)/\left\{4\lambda^{1/2}\,\gamma[2K^2n/(2+n)]^{(3+n)/(2+n)}\right\}$,

W = width of building,

λ and γ = constants of order one that are adjusted to give optimum agreement between theoretical and experimental results,

K = von Karman constant (0.41),

C_{Fx} = force coefficient of building = force/$(0.5\rho\overline{U}(H)\overline{U}(H)WH)$,

$$F_1(z'', y'') = \frac{\eta^{1/(2+n)}\exp\left\{-[\eta + y''^2/(1.5+\eta)]\right\}}{(\eta + 1.5)^{1/2}},$$

$$z'' = (z/H)/[(x-a)/H]^{1/(2+n)},$$

$$\eta = z''^{(2+n)}/[2(2+n)\,K^2n\,\gamma],$$

$$y'' = \frac{(y/H)}{[(x-a)/H]^{1/(2+n)}}\left(\frac{2+n}{2\lambda\gamma K^2 n}\right)^{1/(2+n)}.$$

Thus, for the wake of a three-dimensional building and small n, Hunt's theory predicts that the mean velocity defect decays as $x^{-1.5}$. The same theory predicts that the turbulent intensity excess decays as x^{-2}.

The measurements of Peterka and Cermak [9] do not confirm the existence of the Gaussian distribution of velocity defect in the cross-wind direction incorporated in Hunt's theory [13]. They concluded that this was the result of the well-known horseshoe vortex, which forms in the stagnation region at the front of the building and curls around the building, to produce mean vorticity with its axis in the longitudinal direction. Hunt [14] subsequently developed a vortex-wake theory to account for the effect of horseshoe vortices.

Figure 2 illustrates the various regions of influence. The horseshoe vortex

transfers higher-momentum, less-turbulent fluid downward from elevated portions of the turbulent boundary layer, which increases mean velocity and decreases turbulent intensity near ground level along the centerline of the building.

The longitudinal velocity excess due to a vortex in region E, the inviscid zone, was estimated by Hunt [14] to be

$$u = \frac{n\Gamma\, hy'x}{\pi}\left[\frac{1}{(y'^2 + h^2 + z^2)^2 - 4z^2h^2}\right] \tag{2.2}$$

where $y' = y_v - y$, y_v and h are the distances to the center of the imposed vortex in lateral and vertical directions respectively, and Γ is the circulation at $x = 0$. An interesting feature of eqn. (2.2) is that the velocity excess increases linearly with x in region E. However, this increase cannot persist indefinitely. Hunt [14] concluded that eqn. (2.2) is no longer applicable, once the width of the viscous core, V_+, is approximately equal to y, or the depth of the viscous region G equals z.

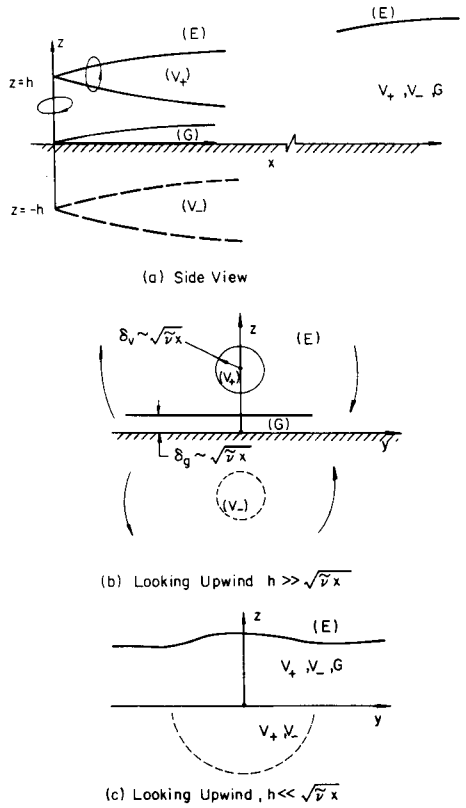

Fig. 2. Schematics of the regions of influence of the vortex core and the vortex-induced boundary layer (from the vortex wake theory of Hunt [14]).

3. Analytical prediction of mean temperature in wake of a building

The physics of vortex and momentum wakes can be applied to any passive scalar such as temperature. In this section, the theory is developed to predict the time-mean temperature field behind a three-dimensional bluff body, deeply immersed in a turbulent stably stratified boundary layer. Some of the expressions developed for the velocity field from Hunt's vortex wake theory [14] are used to derive the present model for the temperature field.

Transport of the scalar quantity temperature is governed by the energy equation. Assuming that the dissipation term is small, and that molecular diffusivity is small compared with eddy diffusivity, the energy equation reduces to

$$\overline{U}\frac{\partial \overline{T}}{\partial x} + \overline{V}\frac{\partial \overline{T}}{\partial y} + \overline{W}\frac{\partial \overline{T}}{\partial z} = \frac{\partial}{\partial x}\left[\epsilon_1 \frac{\partial \overline{T}}{\partial x}\right] + \frac{\partial}{\partial y}\left[\epsilon_2 \frac{\partial \overline{T}}{\partial y}\right] + \frac{\partial}{\partial z}\left[\epsilon_3 \frac{\partial \overline{T}}{\partial z}\right] \tag{3.1}$$

where:

$\overline{U}, \overline{V}, \overline{W}$ = mean velocity components in x, y, and z directions,
$\overline{T}$ = mean temperature,
ϵ_1, ϵ_2 and ϵ_3 = eddy diffusivity in x, y, and z directions.

3.1. Solution of the energy equation in a momentum wake

A building alters the approach flow temperature profile, producing temperature perturbations in the building wake. The perturbed temperature profile diffuses back to the original boundary-layer form in the far wake region. If the temperature stratification is not too strong, then the temperature structure has only a small influence on the flow structure. In this case, the convection and diffusion of the temperature perturbation are similar to those of the velocity perturbation, and an analytical prediction using parallel arguments is possible.

Let $\bar{U}_w$, $\bar{V}_w$, and $\bar{W}_w$ be the mean velocity components in the x, y, and z directions respectively, and let $\bar{T}_w$ be the mean temperature in the wake. Also let $(\bar{U}(x, z), 0, 0)$ be the mean components of velocity, and let $\bar{T}(x, z)$ be the mean temperature in the undisturbed boundary layer. Thus

$$\begin{aligned} \overline{U}_w &= \overline{U}(x, z) + u(x, y, z) \\ \overline{V}_w &= v(x, y, z) \\ \overline{W}_w &= w(x, y, z) \\ \overline{T}_w &= \overline{T}(x, z) + \theta(x, y, z) \end{aligned} \tag{3.2}$$

where u, v, w and θ are the building-induced perturbations of the three mean velocity components and the mean temperature, respectively. The assumptions $|u|/\overline{U} \ll 1$ and $|\theta|/\overline{T} \ll 1$ imply that the present analysis is valid only far downstream of the body (perhaps $5H$) where perturbations are small. Combination of eqn. (3.1) with eqns. (3.2), when the terms for the undisturbed

boundary layer are removed, results in the perturbation equation:

$$\overline{U}\frac{\partial\theta}{\partial x} + u\frac{\partial\overline{T}}{\partial x} + u\frac{\partial\theta}{\partial x} + v\frac{\partial\overline{T}}{\partial y} + v\frac{\partial\theta}{\partial y} + w\frac{\partial\overline{T}}{\partial z} + w\frac{\partial\theta}{\partial x}$$
$$= \frac{\partial}{\partial x}\left(\epsilon_1\frac{\partial\theta}{\partial x}\right) + \frac{\partial}{\partial y}\left(\epsilon_2\frac{\partial\theta}{\partial y}\right) + \frac{\partial}{\partial z}\left(\epsilon_3\frac{\partial\theta}{\partial z}\right) \tag{3.3}$$

The continuity equation for the perturbation quantities is given by

$$\frac{\partial u}{\partial x} + \frac{\partial y}{\partial y} + \frac{\partial w}{\partial z} = 0 \tag{3.4}$$

L is the distance over which the wake extends, and l is a length scale in the x direction (say the separated region length); hence $l \ll L$. The thickness, Δ, and width, d, of the wake are assumed to be of the same order of magnitude. The gradients of u, v and w with respect to x, y and z, respectively, are of the same order of magnitude. Hence, each term of eqn. (3.4) is proportinal to the other, and given by

$$v \sim \frac{ud}{l} \quad \text{and} \quad w \sim \frac{u\Delta}{l} \tag{3.5}$$

Let $\overline{U}_0$ and $\overline{T}_0$ be the mean velocity and temperature at $z = \Delta$ in the undisturbed boundary layer. Assuming $|\theta|/\overline{T}_0 \ll 1$ and $|u|/\overline{U}_0 \ll 1$, the order of magnitude of each term of eqn. (3.3) was determined. Dropping terms of smaller size, and noting that $\overline{T}$ is not a function of y and that $l > \Delta$ or d, eqn. (3.3) reduces to

$$\overline{U}\frac{\partial\theta}{\partial x} + w\frac{\partial\overline{T}}{\partial z} = \frac{\partial}{\partial y}\left(\epsilon_2\frac{\partial\theta}{\partial y}\right) + \frac{\partial}{\partial z}\left(\epsilon_3\frac{\partial\theta}{\partial z}\right) \tag{3.6}$$

$\overline{T}$ can be expressed by a power-law profile, with exponent $n_2 \ll 1$, as,

$$\frac{\overline{T}}{\overline{T}_0} = \left(\frac{z}{\Delta}\right)^{n_2} \tag{3.7}$$

Therefore,

$$w\frac{\partial\overline{T}}{\partial z} = \frac{w\overline{T}_0 n_2}{\Delta^{n_2}}(z)^{n_2-1} \approx \left(\frac{u\Delta}{l}\right)\left(\frac{\overline{T}_0 n_2}{\Delta}\right) \approx \frac{u\theta}{l} \ll \frac{\overline{U}_0\theta}{l}$$

may also be neglected compared with the other terms of eqn. (3.6) to give

$$\overline{U}\frac{\partial\theta}{\partial x} = \frac{\partial}{\partial y}\left(\epsilon_2\frac{\partial\theta}{\partial y}\right) + \frac{\partial}{\partial z}\left(\epsilon_3\frac{\partial\theta}{\partial z}\right) \tag{3.8}$$

Further analysis is based on constant eddy transport coefficients ϵ_2 and ϵ_3, given by $\epsilon_3 = \gamma\bar{\epsilon}$ and $\epsilon_2 = \lambda\epsilon_3 = \lambda\gamma\bar{\epsilon}$, where λ and γ are constants of order one and $\bar{\epsilon}$ is the constant eddy transport coefficient. The assumption of constant eddy transport coefficients was used to permit an analytical solution, and because Lemberg's [7] incorporation of a variable eddy coefficient into the momentum wake solution provided only minor improve-

ment. The assumption of constant eddy diffusivity linearizes eqn. (3.8), and the solution can be directly obtained. The power-law profile for the undisturbed velocity boundary layer, $n \ll 1$, is given by,

$$\frac{\overline{U}}{\overline{U}_0} = \left(\frac{z}{\Delta}\right)^n \tag{3.9}$$

A length scale c_1 equal to $(\epsilon_3 \Delta^n / \overline{U}_0)^{1/(1+n)}$, proportional to the height of the building, was used to nondimensionalize x, y, and z variables. Hence with $\bar{x} = x/c_1$, $\bar{y} = y/c_1$, $\bar{z} = z/c_1$, eqn. (3.8) reduces to,

$$\bar{z}^n \frac{\partial \theta}{\partial \bar{x}} = \lambda \frac{\partial^2 \theta}{\partial \bar{y}^2} + \frac{\partial^2 \theta}{\partial \bar{z}^2} \tag{3.10}$$

Hinze [15] states that ϵ_3 is of the same order as eddy viscosity $\bar{\nu}$. Arya [16] calculated the ratio of $\epsilon_3/\bar{\nu}$ for the fully developed undisturbed turbulent boundary layer, and he found that the ratio is approximately equal to 0.85. Thus the following was assumed,

$$\epsilon_3 = \gamma \bar{\epsilon} = 0.85\, \gamma \bar{\nu} \text{ and } \epsilon_2 = 0.85\, \lambda \gamma \bar{\nu} \tag{3.11}$$

The eddy viscosity was calculated from the parameters of the undisturbed boundary layer neglecting advection and diffusion, the details of which are discussed by Hunt and Smith [4].

Equation (3.10) has the form of a diffusion equation. The solution procedure adopted is similar to that of Smith [17], and further details are given by Kothari [18].

The solution of eqn. (3.10) may be assumed to be of the form

$$\theta(x, y, z) = \mathrm{F}(\bar{x}, \bar{z}) \exp\left[-\bar{y}^2/\mathrm{f}(\bar{x}, \bar{z})\right] \tag{3.12}$$

Functions $\mathrm{F}(\bar{x}, \bar{z})$ and $\mathrm{f}(\bar{x}, \bar{z})$ are evaluated using the technique of Smith [17]:

$$\mathrm{F}(\bar{x}, \bar{z}) = q_0 \sqrt{q_0/(2\pi q_2)} \text{ and } \mathrm{f}(\bar{x}, \bar{z}) = 2q_2/q_0 \tag{3.13}$$

where

$$q_0(\bar{x}, \bar{z}) = \int_{-\infty}^{\infty} \theta \, \mathrm{d}\bar{y} \text{ and } q_2(\bar{x}, \bar{z}) = \int_{-\infty}^{\infty} \bar{y}^2 \theta \, \mathrm{d}\bar{y} \tag{3.14}$$

The functions q_0 and q_2 are the solutions of the following differential equations (see Hunt and Smith [4]):

$$\bar{z}^n \frac{\partial q_0}{\partial \bar{x}} = \frac{\partial^2 q_0}{\partial \bar{z}^2} \tag{3.15}$$

and

$$\bar{z}^n \frac{\partial q_2}{\partial \bar{x}} = \frac{\partial^2 q_2}{\partial \bar{z}^2} + 2\lambda q_0 \tag{3.16}$$

with boundary conditions,

$$q_0 = q_2 = 0 \text{ at } \bar{z} = 0 \text{ and } \bar{z} \to \infty$$
$$q_0 = q_2 = 0 \text{ at } \bar{y} \to -\infty \text{ and } \bar{y} \to +\infty \tag{3.17}$$

and

$$\int_{-\infty}^{\infty} \left(\int_{0}^{\infty} z\overline{U}\theta \, d\bar{z} \right) d\bar{y} = \bar{c}$$

where $\bar{c}$ is a constant. One expects the building to mix the temperature profile across the wake, so that with appropriate approximations, $\bar{c} \approx H\overline{T}(H)\overline{U}(H)$.

The solution of eqns. (3.15) and (3.16) with boundary conditions given by eqn. (3.17) was obtained using the method of Smith [17]. With eqn. (3.13), the functions $F(\bar{x}, \bar{z})$ and $f(\bar{x}, \bar{z})$ were then evaluated. The perturbation temperature defect θ is given by

$$\frac{\theta(x, y, z)}{\text{DELTA } T} = k_2 \frac{\overline{T}(H)}{\text{DELTA } T} \frac{F_2(z'', y'')}{\left(\frac{x-a}{H}\right)^{(3+n)/(2+n)}} \tag{3.18}$$

where:

DELTA T = $\overline{T}_\delta - \overline{T}_{z_1}$ in the undisturbed boundary layer used for nondimensionalization,

$\overline{T}_\delta$ = mean temperature at the top of the turbulent boundary layer,

$\overline{T}_{z_1}$ = mean temperature at the reference height z_1,

$\overline{T}(H)$ = mean temperature at the building height in the undisturbed flow,

k_2 = constant to be determined by matching with the experimental result,

a = virtual origin of the wake to be determined from experiment,

n = boundary layer velocity profile power-law exponent,

$$F_2(z'', y'') = \frac{\eta^{1/(2+n)}}{(\eta + 1.5)^{1/2}} \exp\left[-\left(\eta + c_8 \frac{y''^2}{(\eta + 1.5)} \right) \right],$$

$$z'' = \frac{(z/H)}{\left[\frac{x-a}{H}\right]^{1/(2+n)}},$$

$$\eta = \frac{z''^{(2+n)}}{[2(2+n)\, K^2 n\, 0.85\, \gamma]},$$

$$y'' = \frac{(y/H)}{\left[\frac{x-a}{H}\right]^{1/(2+n)}} \left[\frac{(2+n)}{2\lambda\, 0.85\, \gamma\, K^2 n} \right]^{1/(2+n)},$$

K = von Karman constant (0.41),

c_8 = constant to be determined from experimental results. However, along the building centerline $y'' = 0$ and hence coefficient c_8 does not play any role.

3.2. Solution of the energy equation in a vortex wake

During the analysis of a momentum wake behind a surface obstacle as described in Section 3.1, it was assumed that trailing vortices are weak, and, hence, do not affect wake perturbations. However, the experiments by Hansen et al. [8], Hansen and Cermak [10], and Woo et al. [3] on the wakes behind hemispheres and cubes have shown that vortices may persist, and they have significant effects on the wake structure.

To analyze the effect of a bound vortex on the temperature field behind a bluff body, the effect of perturbations in vertical velocity must be considered. Equation (3.6) is the starting point for a vortex wake analysis of temperature perturbation,

$$\overline{U}\frac{\partial\theta}{\partial x} + w\frac{\partial\overline{T}}{\partial z} = \epsilon_2\frac{\partial^2\theta}{\partial y^2} + \epsilon_3\frac{\partial^2\theta}{\partial z^2} \tag{3.19}$$

The perturbations u, v, w, and θ expressed as an asymptotic expression in powers of n are,

$$\begin{aligned} u &= u^{(0)} + nu^{(1)} + \ldots \\ v &= v^{(0)} + nv^{(1)} + \ldots \\ w &= w^{(0)} + nw^{(1)} + \ldots \\ \theta &= \theta^{(0)} + n\theta^{(1)} + \ldots \end{aligned} \tag{3.20}$$

where $u^{(0)}$, $v^{(0)}$, $w^{(0)}$, $\theta^{(0)}$ and $u^{(1)}$, $v^{(1)}$, $w^{(1)}$, $\theta^{(1)}$ are all of order unity. The superscript indicates the power of n by which the perturbation quantity is multiplied. Thus, eqn. (3.20) represents the descending series of perturbation quantities u, v, w, and θ. The undisturbed boundary layer mean velocity $\overline{U}$ and mean temperature $\overline{T}$ and their derivatives $\partial\overline{U}/\partial z$ and $\partial\overline{T}/\partial z$ expressed in terms of asymptotic series of power-law exponents n and n_2, respectively, with assumptions $n \ll 1$ and $n_2 \ll 1$, are

$$\overline{U} = \overline{U}(h)\, e^{n\ln(z/h)} \tag{3.21}$$

$$\overline{U} = \overline{U}(h)\,[1 + n\ln(z/h) + \frac{n^2}{2!}(\ln z/h)^2 + \ldots] \tag{3.22}$$

$$\frac{\partial\overline{U}}{\partial z} = \frac{n}{z}\overline{U}(h)\,[1 + n\ln(z/h) + \ldots] \tag{3.23}$$

$$\overline{T} = \overline{T}(h)\, e^{n_2\ln(z/h)} \tag{3.24}$$

$$\overline{T} = \overline{T}(h)\,[1 + n_2\ln(z/h) + \frac{n_2^2}{2!}(\ln z/h)^2 + \ldots] \tag{3.25}$$

and

$$\frac{\partial \overline{T}}{\partial z} = \frac{n_2 \overline{T}(h)}{z} [1 + n_2 \ln(z/h) + \ldots.] \tag{3.26}$$

Using the assumption of $n_2 \approx n$, eqns. (3.25) and (3.26) can be written as,

$$\overline{T} = \overline{T}(h) [1 + n \ln(z/h) + \frac{n^2}{2!} (\ln z/h)^2 + \ldots] \tag{3.27}$$

$$\frac{\partial \overline{T}}{\partial z} = \frac{n}{z} \overline{T}(h) [1 + n \ln(z/h) + \ldots] \tag{3.28}$$

Hunt [14] concluded that for region E (Fig. 2), the zeroth order perturbation velocity field is irrotational. He also concluded that $u^{(0)}$ is zero everywhere, and he determined that

$$w^{(0)} = \frac{\Gamma}{4\pi} \left[- \frac{y'}{y'^2 + (z-h)^2} + \frac{y'}{y'^2 + (z+h)^2} \right] \tag{3.29}$$

for

$$x/h \gg \frac{\sqrt{4x\bar{\nu}/\bar{U}(h)}}{h} \text{ and } y' = y_v - y$$

where y_v and h are the lateral and vertical distances from the x axis to the center of a vortex, respectively, and Γ is the circulation of vortex at $x = 0$. Substitution of eqns. (3.20) through (3.28) in eqn. (3.19) gives

$$\overline{U}(h) [1 + n \ln(z/h)] \frac{\partial}{\partial x} (\theta^{(0)} + n\theta^{(1)}) + (w^{(0)} + nw^{(1)}) \frac{n}{z} \overline{T}(h) [1 + n \ln(z/h)]$$

$$= \epsilon_2 \frac{\partial^2 (\theta^{(0)} + n\theta^{(1)})}{\partial y^2} + \epsilon_3 \frac{\partial^2 (\theta^{(0)} + n\theta^{(1)})}{\partial z^2} \tag{3.30}$$

Now, comparing the coefficients of n^0 and n^1 in eqn. (3.30), the following equations are obtained:

$$\overline{U}(h) \frac{\partial \theta^{(0)}}{\partial x} = \epsilon_2 \frac{\partial^2 \theta^{(0)}}{\partial y^2} + \epsilon_3 \frac{\partial^2 \theta^{(0)}}{\partial z^2} \tag{3.31}$$

$$\overline{U}(h) \frac{\partial \theta^{(1)}}{\partial x} + \overline{U}(h) \ln(z/h) \frac{\partial \theta^{(0)}}{\partial x} + \frac{\overline{T}(h)}{z} w^{(0)}$$

$$= \epsilon_2 \frac{\partial^2 \theta^{(1)}}{\partial y^2} + \epsilon_3 \frac{\partial^2 \theta^{(1)}}{\partial z^2} \tag{3.32}$$

For the inviscid region E, it is known that as $\nu \approx 0$, $\epsilon_3 = \gamma\bar{\epsilon} = 0.85\,\gamma\bar{\nu} \approx 0$ and $\epsilon_2 = \lambda\gamma\bar{\epsilon} = 0.85\lambda\gamma\bar{\nu} \approx 0$. Hence, ϵ_3 and ϵ_3 are assumed zero in the region E, which produces the simplified equations,

$$\frac{\partial \theta^{(0)}}{\partial x} = 0 \tag{3.33}$$

$$\overline{U}(h)\frac{\partial\theta^{(1)}}{\partial x} + \frac{\overline{T}(h)}{z}w^{(0)} = 0 \tag{3.34}$$

Since, $\theta^{(0)} \to 0$ as $x \to -\infty$ and since $w^{(0)}$ only induces the temperature perturbation of $0(n)$ as shown by eqn. (3.34), it can be concluded from eqn. (3.33) that $\theta^{(0)}$ is zero everywhere. Integrating eqn. (3.34) with respect to x:

$$\theta^{(1)} = -\frac{\overline{T}(h)}{\overline{U}(h)}\int_0^x \frac{w^{(0)}}{z}\,dx \tag{3.35}$$

Now, substituting for $w^{(0)}$ from eqn. (3.29), the perturbation temperature $\theta^{(1)}$ is,

$$\theta^{(1)} = \frac{\Gamma h y' x}{\pi}\left[\frac{1}{(y'^2 + h^2 + z^2)^2 - 4z^2h^2}\right]\frac{\overline{T}(h)}{\overline{U}(h)} \tag{3.36}$$

Hence, noting that $\theta^{(0)} = 0$, the perturbation temperature excess is given by,

$$\theta = \frac{n\Gamma h y' x}{\pi}\left[\frac{1}{(y'^2 + h^2 + z^2)^2 - 4z^2h^2}\right]\frac{\overline{T}(h)}{\overline{U}(h)} \tag{3.37}$$

Equation (3.37) was doubled in the calculation to account for the presence of two parallel vortices. The total excess perturbation temperature θ is given by the algebraic sum of eqn. (3.18) and twice eqn. (3.37).

4. Experimental measurements

All measurements were performed in the meteorological wind tunnel shown in Fig. 3 at the Fluid Dynamics and Diffusion Laboratory, Colorado State University. It is a closed circuit facility with 9:1 contraction ratio; the test section is 1.83 m (6 ft.) square and 26.8 m (88 ft.) in length, with an adjustable roof to obtain zero pressure gradient along the test section. A 3.8 cm (1.5 in.) high sawtooth was installed at the test section entrance to ensure prompt formation and growth of the boundary layer. The wind tunnel permits independent control of the floor temperature and air temperature. Atmospheric boundary-layer simulation criteria have been discussed by Cermak [19], and Cermak and Arya [20]. A slightly stable boundary layer was developed to determine its influence on wake structure. Table 1 shows the dimensions of the various buildings tested and the characteristics of the approach boundary layer. The temperature at the ground was always maintained at 0°C (32°F) by means of a refrigeration circuit. All velocity defect and temperature excess values were calculated by finding the differences between velocity or temperature at a point in the wake and the velocity or temperature at the same point in the absence of the building. A series of wake measurements were made at x/H values of 1.0, 2.5, 5.0, 7.5, 10.0, 15.0, 20.0, 30.0, 40.0, and 60.0 at various z/H locations for

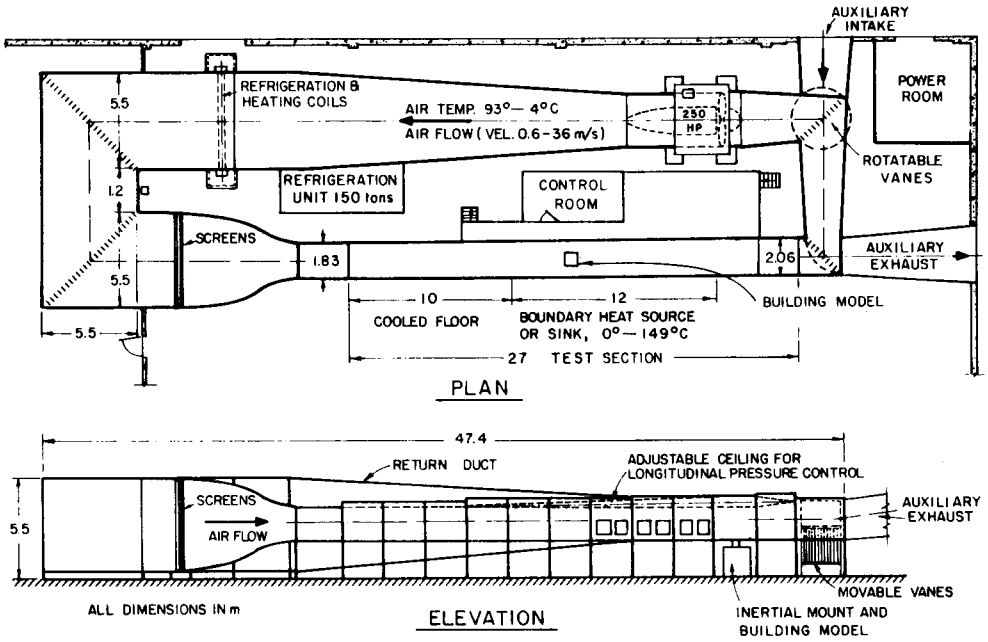

Fig. 3. Meteorological wind tunnel, Fluid Dynamics and Diffusion Laboratory, Colorado State University.

$y/H = 0.0$, with and without the building in place. The results for building 3 are reported herein, however, similar results were obtained for other buildings; details are given by Kothari [18].

Measurements of mean and fluctuating velocity and temperature in the building wake were made using two parallel hot-film sensors, each operated at a different, but constant temperature. Calibrations of the films in a set of flows in which both velocity and temperature were made to vary using a variable-exponent King's law of the form

$$\frac{E^2}{R(R - R_a)} = A + B\,U^c \tag{4.1}$$

This formulation specified both velocity and temperature in the turbulent boundary layer flow. Calculation of T and U was performed at each time increment from digital records of the hot-films voltage outputs. Digitization was at 250 samples per second. The time series of T and U thus obtained were used to calculate the root mean square values T_{rms} and u_{rms} and mean quantities $\overline{T}$ and $\overline{U}$. Calibrations of the hot films were performed daily. Analysis of measurement accuracy, supported by repeatability measurements, indicated that accuracy is within 10% for flow with turbulence intensity less than 20—30%. Accuracies in general decrease steadily with increasing turbulence intensity. Measurements in the presence of 50% turbulence intensity should be considered semi-quantitative.

TABLE 1

Building model dimensions, boundary layer parameters and constants

Building	Height H (cm)	Width W (cm)	Depth D (cm)	$\overline{U}(\delta)$ ($m\,s^{-1}$)	$\overline{U}(H)$ ($m\,s^{-1}$)	$\overline{T}(\delta)$ (°C)	$\overline{T}(H)$ (°C)	$\frac{u_*}{\overline{U}(H)}$	$\frac{z_0}{H}$	Re_H	Ri_δ	Ri_H	C_{Fx}	k_2	a/H	$\Gamma_x = 0$ ($m^2\,s^{-1}$)
1	6.25	4.88	15.88	5.96	4.26	47.19	36.89	0.053	5.6×10^{-3}	2.1×10^{4}	0.0229	4.6×10^{-3}	1.30	11.3	−2.50	0.45
2	6.25	15.88	4.88	5.96	4.26	47.19	36.89	0.053	5.6×10^{-3}	2.1×10^{4}	0.0229	4.6×10^{-3}	1.40	13.1	−1.75	1.44
3	7.62	7.62	7.62	5.67	4.27	44.16	35.18	0.053	4.6×10^{-3}	2.5×10^{4}	0.0235	5.0×10^{-3}	1.30	8.7	−0.30	0.71
4	10.16	5.08	10.16	5.85	4.74	45.51	38.01	0.047	3.4×10^{-3}	3.7×10^{4}	0.0227	5.8×10^{-3}	1.35	5.5	−1.35	0.49
5	10.16	10.16	5.08	5.85	4.74	45.51	38.01	0.047	3.4×10^{-3}	3.7×10^{4}	0.0227	5.8×10^{-3}	1.35	8.5	−1.50	1.0
6	10.16	10.16	10.16	5.85	4.74	45.51	38.01	0.047	3.4×10^{-3}	3.7×10^{4}	0.0227	5.8×10^{-3}	1.30	8.6	−1.0	1.0

Boundary layer height = 50.8 cm.
$\overline{U}_{z_1} = 1.68\ m\,s^{-1}$, $\overline{T}_{z_1} = 21.1°C$ at reference height of 0.25 cm.
Average mean velocity profile power-law index, $n = 0.16$.
$\lambda = 1.0$, $\gamma = 1.0$.

5. Results and discussions

Detailed wake measurements for one wind direction, viz. one face perpendicular to the flow, were obtained in preference to a series of less-detailed measurements at many wind directions. Figure 4 shows the approach flow characteristics. The lower reference temperature, $\overline{T}_{z_1}$, and lower reference velocity, $\overline{U}_{z_1}$, were at the height $z_1 = 0.25$ cm, and were equal to 21.1°C (70°F) and 1.68 m s^{-1} (5.5 ft./s), respectively. The bulk gradient Richardson number calculated across the boundary layer, from z_1 to the outer edge of the boundary layer z_2, was 0.023. The bulk Richardson number between z_1 and the height of the building was about 0.005.

The mean velocity defect, Delta U, the turbulence variance excess, Delta U VAR, the mean temperature excess, Excess T, and the temperature variance excess, Delta T VAR, are defined as follows:

$$\text{Delta } U = \left(\frac{\overline{U}(z)}{\overline{U}(\delta)}\right)_{\text{without building}} - \left(\frac{\overline{U}(z)}{\overline{U}(\delta)}\right)_{\text{with building}},$$

$$\text{Delta } U\text{VAR} = \left(\frac{u_{\text{rms}}(z)}{\overline{U}(z)}\right)^2_{\text{with building}} - \left(\frac{u_{\text{rms}}(z)}{\overline{U}(z)}\right)^2_{\text{without building}},$$

$$\text{Excess } T = \frac{\overline{T}(z)_{\text{with building}} - \overline{T}(z)_{\text{without building}}}{\text{DELTA } T},$$

$$\text{Delta } T\text{ VAR} = \frac{T^2_{\text{rms}}(z)_{\text{with building}} - T^2_{\text{rms}}(z)_{\text{without building}}}{(\text{DELTA } T)^2}$$

$$\text{Delta } T = (\overline{T}(\delta) - \overline{T}_{z_1})_{\text{without building}}$$

$\overline{T}(\delta)$ = mean temperature at the top of the turbulent boundary layer,

$\overline{T}_{z_1}$ = mean temperature at reference height z_1,

δ = turbulent boundary layer thickness, and

$u_{\text{rms}}(z)$ and $T_{\text{rms}}(z)$ are the root-mean-square (rms) of velocity and temperature at height z, respectively.

5.1. Experimental measurements of mean velocity in the wakes of buildings

Figure 5 shows the vertical profiles of mean velocity defect, Delta U, for building 3. The maximum vertical extent of the velocity defect wake is 2 to 3H for the entire wake and is of the same order of magnitude as reported by Woo et al [3]. Large fluctuations in velocity and temperature at $x/H = 1.0$ and 2.5 reduce the accuracy of velocity and temperature measurements (the hot-film anemometer is incapable of distinguishing negative velocity from positive velocity in the separated flow region). The wake extends much further downstream than those reported by Counihan [5], Colmer [1], Lemberg [7], and Castro and Robins [6]. However, the downwind extent of the wakes behind the buildings does agree with the results of Hansen et al. [8,10] and Woo et al. [3]. The momentum wake dissipated in about 10 to

15H downstream of the building; however, the effect of the vortex wake persisted to at least 60H downstream of the building. The measurements were not performed beyond a distance of 60H downstream; hence, the total length of the wake is not known. The horseshoe vortices transfer

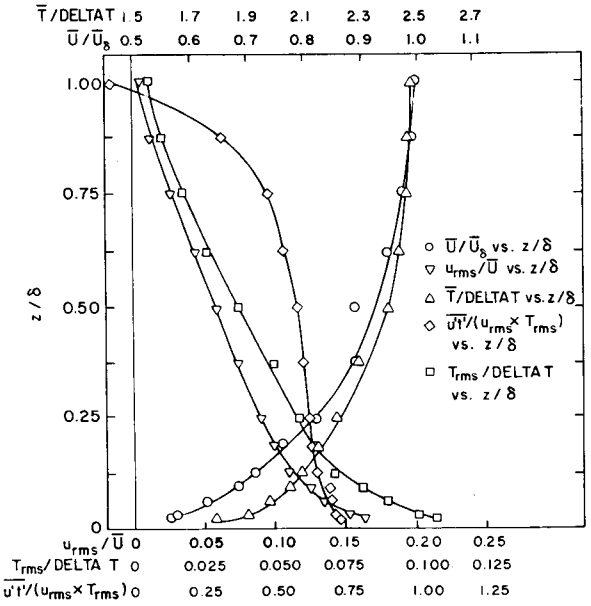

Fig. 4. Approach flow characteristics.

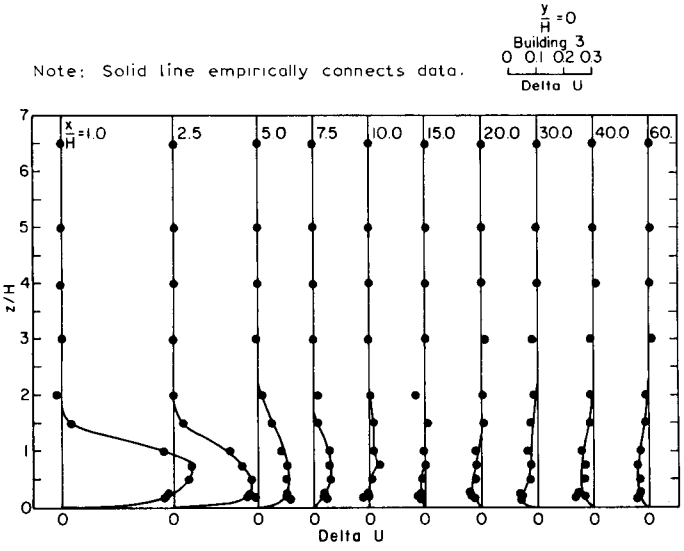

Fig. 5. Vertical profiles of mean velocity defect behind building 3.

higher momentum fluid from the top of the boundary layer into the wake region, which increases mean velocity along the wake centerline. The vortices result in excess velocity within the far wake region (hence the negative velocity defect).

The maximum velocity defect for each x/H for building 3 is shown in Fig. 6. This maximum velocity defect did not occur at the same z/H for each x/H value. The mean velocity defect decays with a power-law exponent of −1.65. The theory for neutrally stable wakes proposed by Hunt and Smith [4] would predict a power-law decay of about −1.5. A decay rate higher than −1.5 results from the action of two longitudinal vortices which transport higher momentum fluid down toward the surface on the centerline. Examination of Fig. 5 shows that these decay curves actually go negative before approaching zero. Thus, the high power-law exponent does not necessarily imply a rapid dissipation of the wake. The horseshoe vortex is more dominant in a stably stratified flow than it is in the neutral case; hence, neither the theory of a momentum wake nor the power-law decay description of the wake maximum velocity defect is really appropriate. The neutral flow data of Woo et al. [3] have been included in Fig.6 for comparison.

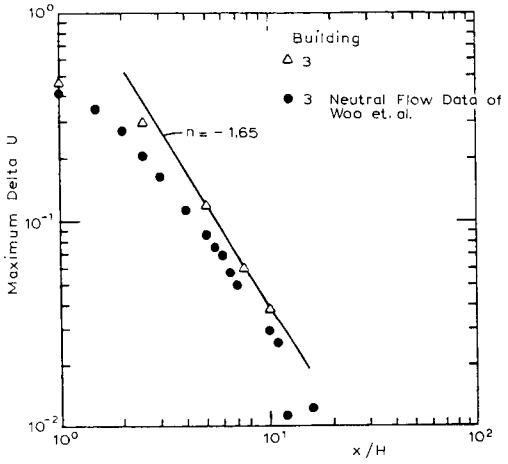

Fig. 6. Comparison of decay rate of mean velocity defect in the wake of building 3 with Woo et al. [3].

5.2. Comparison of the experimental measurements of mean velocity with Hunt's theories

The theory of wakes behind buildings deeply immersed in a turbulent boundary layer was reviewed in Section 2.3. The theory requires knowledge of the force coefficient, C_{Fx}. Values of force coefficients were derived from the measurements of Akins et al. [21]; for building 3, $C_{Fx} = 1.3$. The constants λ and γ in Hunt's theory were assumed equal to one for all the calculations. The virtual origin, a, for the building wake was determined from

the variation of the experimental data along the wake centerline and was found equal to $-0.3H$ for building 3. The theoretical predictions of mean velocity defect for the momentum wake theory of Hunt [13] were then calculated using eqn. (2.1). The vertical profiles of the mean velocity defect, Delta U, due to the momentum wake for various x/H locations are shown in Fig. 7. The mean velocity excess observed in the wake is never predicted by the momentum wake theory.

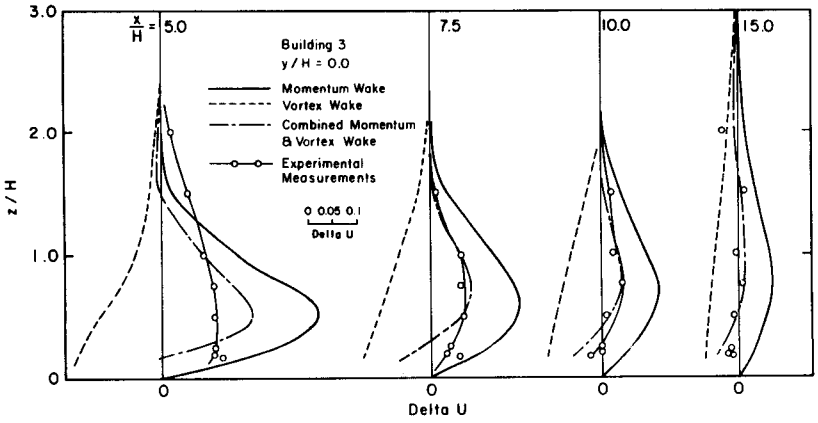

Fig. 7. Comparison of the measured vertical profiles of velocity defect on the building 3 centerline with the momentum and vortex wake theory of Hunt [14].

Calculation of the influence of the longitudinal vorticity using the model of Section 2.3 required both the position of the vortex in the wake and the circulation, Γ, at $x = 0$. The results of Hansen and Cermak [10] have shown that the vortex moves laterally and vertically with increasing x. In the present calculations, the observed values of y_v, the lateral center of each vortex, were obtained from the measurements of Hansen and Cermak [10] behind hemispheres. The height of the center of each vortex, h, was assumed constant and equal to $0.3H$ [3,8,10].

The following technique was developed to evaluate the circulation at $x = 0$. It was assumed that part of the circulation in the approach flow is converted into the circulation of the horseshoe vortex. The circulation in the approach flow, Γ_a, up to the height z, is given by $\overline{U}(\delta)x_L(z/\delta)^n$ where x_L is a reference length. When calculating the strength of the horseshoe vortex, a value of z equal to $0.3H$ was found to provide a consistence comparison with experimental data for a variety of buildings. The horseshoe vortex in front of the building is presumed to roll like a circular tube. The diameter of this tube was assumed as $0.8W$ [3,8,10], where W is the width of the building. The reference length, x_L, was chosen as the circumference of this tube and is euqal to $\pi(0.8W)$. Using this method, $\Gamma_{x=0}$ for building 3 was calculated to be 0.71 $m^2 s^{-1}$ (7.6 $ft.^2/s$). The results of the calculations of the vortex wake using eqn. (2.2), along the centerline of the building for various x/H are also shown in Fig. 7.

The sum of the momentum wake velocity defect and the vortex wake velocity excess are displayed in Fig. 7, along with the experimental observations of velocity defect in the wake. The comparison between the measurements and the combined momentum- and vortex-wake theory is very satisfactory for x/H greater than 5. The comparisons deteriorate at $x/H = 5.0$ near the separated region (the near-wake region) behind the building as expected. The flow in this region cannot be considered a small perturbation on the approach flow. Comparisons of the theory with experiment beyond $x/H = 15$ were not made for two reasons: (1) decrease in vortex strength with distance through dissipation could be important, and (2) the predicted velocity is somewhat sensitive to the vortex position, y_v, which could not be easily estimated. A reasonable position of the vortex could always be found such that the theory and experiment agreed; however, no independent check of the vortex location was available at large x/H values.

5.3. *Experimental measurements of mean temperature in the wakes of buildings*

Figure 8 shows vertical profiles of mean temperature excess, Excess T, for building 3 with one face normal to the flow direction. The maximum vertical extent of the temperature excess is about 1 to $2H$ in the near wake and 2 to $4H$ in the far wake. The temperature wake extends much farther than the velocity wake. Even at a distance of x/H equal to 60, the measurements confirmed a substantial centerline temperature excess.

The maximum mean temperature excess occurring at each x/H is shown in Fig. 9 for all buildings. This maximum did not occur at the same z/H for the various values of x/H. For all buildings this maximum increases until approximately 8 to $15H$ downstream of the buildings, and then it decreases. Similar increases in the mean temperature magnitudes were reported by

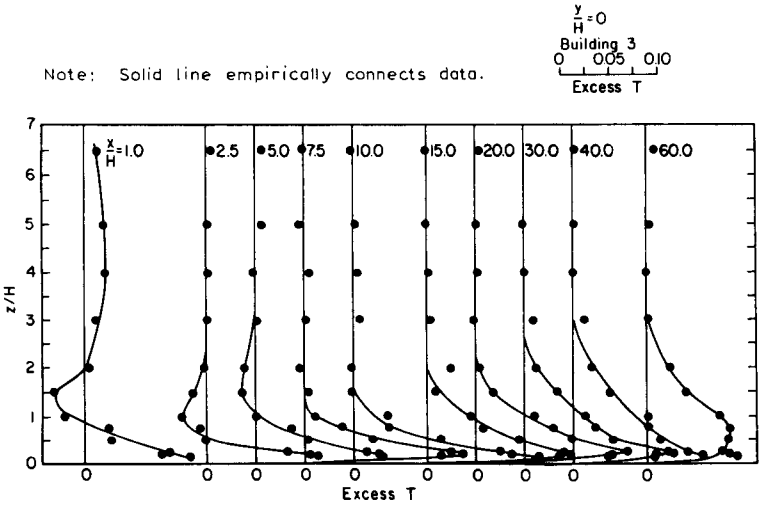

Fig. 8. Vertical profiles of mean temperature excess behind building 3.

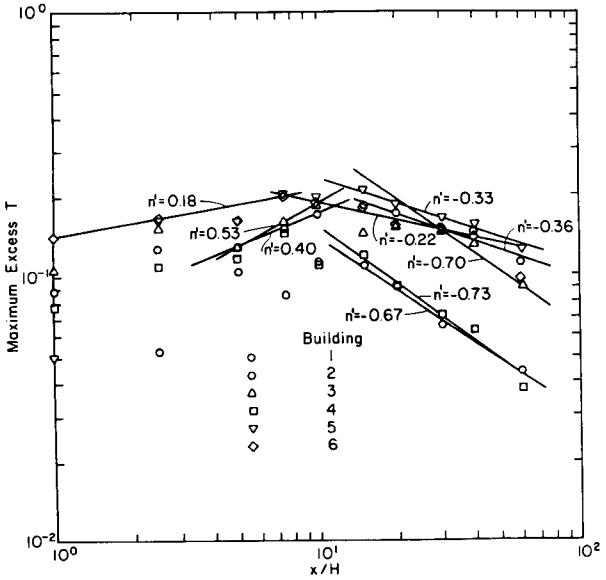

Fig. 9. Variation of mean temperature excess in the wake of buildings.

Alexopoulos and Keffer [22] for off-centerline data in flow behind a cylinder immersed in a uniform flow with a linear temperature gradient. For buildings 2, 3, and 6, the maximum mean temperature excess increases with a power-law exponent of 0.40, 0.53, and 0.18, and then decreases with an exponent of −0.36, −0.70, and −0.22, respectively. For buildings 1, 4, and 5, the initial increase in the form of a power-law exponent was difficult to determine; however, beyond certain x/H the exponents were −0.67, −0.73, and −0.33, respectively. The decay of temperature excess is slower than the decay of velocity defect. Hence, the horseshoe vortices play a more dominant role in a stable temperature wake than in a velocity wake.

5.4. Comparison of the experimental measurements of mean temperature with the present theories

The horseshoe vortex in the region E of a building wake increases the mean temperature on the building wake centerline, as predicted by eqn. (3.37). Calculations for region E were extrapolated into the regions G and V_+, where the assumptions of $\epsilon_3 \approx 0$ and $\epsilon_2 \approx 0$ may not be valid. The action of two horseshoe vortices along the centerline of a building was the same and additive; hence the result of eqn. (3.37) was doubled to obtain the net excess temperature due to vortices. The circulation Γ at $x = 0$ and the position of the vortex were assumed the same as for the velocity calculation. Figure 10 shows the excess temperature due to the vortex behind building 3.

The momentum wake theory for the mean temperature results in a mean temperature defect in the wake behind a building, and it is analogous to the velocity defect in the momentum wake theory of Hunt [13]. The mean

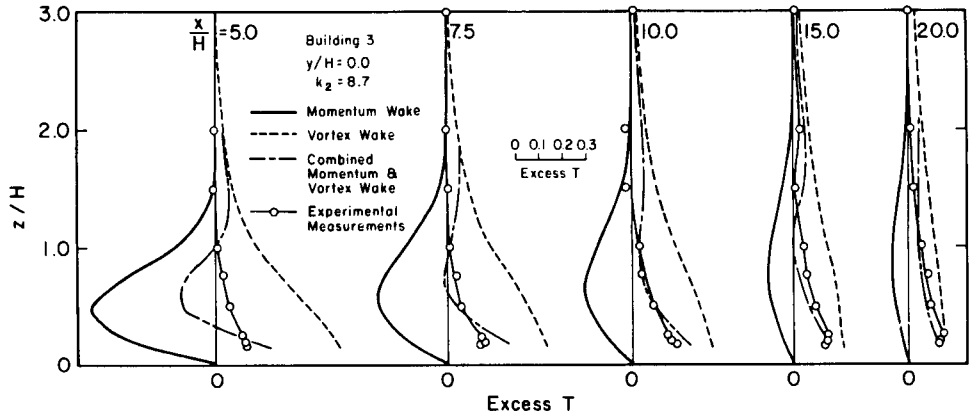

Fig. 10. Comparison of the measured vertical profiles of temperature excess on the building 3 centerline with the present theory.

temperature defect due to the building is given by eqn. (3.18). The constants λ and γ were also assumed equal to one for the mean temperature calculations. It was reasonable to assume that the velocity and temperature wake originates from the same point. Consequently, the virtual origin a for temperature wake is the same as the velocity wake. The constant k_2 in eqn. (3.18) was evaluated by matching the experimental observation of excess temperature on the centerline of each building at $x/H = 10$ and $z/H = 1$ to the sum of excess temperature due to vortex wake given by eqn. (3.37) and the momentum wake temperature defect given by eqn. (3.18). Knowing k_2, the calculations for temperature defect in the wake were performed according to eqn. (3.18), and results of calculations are shown in Fig. 10.

The sum of vortex wake temperature excess and momentum wake temperature defect are also shown in Fig. 10, together with the experimental observations of temperature excess in the wake. The comparison between the measurements and the combined momentum and vortex wake theory is quite good, deviating only near the building, where perturbations are large. The constant k_2 is apparently influenced by the building geometry (see Table 1). The constant k_2 for all buildings of W/H ratio of one was ~8.7. For other shapes, k_2 ranged from 5.5 to 13. Thus, the present theory can provide a reasonable estimate of the thermal wake by using a value of k_2 from Table 1.

The local bulk Richardson number can be evaluated knowing the temperature field behind a building to determine the local stability of the flow field. The local stability tends to move towards a less stable flow than the approach conditions.

5.5. Turbulence measurements

The vertical profiles of turbulence variance excess, Delta U VAR, in the wake of building 3 are shown in Fig. 11. The mean square values of turbulent velocity fluctuation return to the undisturbed state at approximately

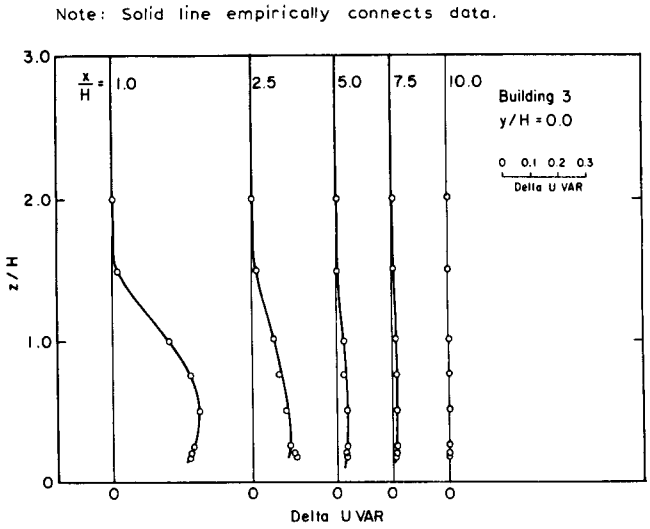

Fig. 11. Vertical profiles of turbulence intensity excess variance on the centerline of building 3.

7.5 to 10H downstream of the building. This return is much more rapid than for the mean velocity field. Similar findings were reported by Peterka and Cermak [9], Hansen et al. [8], and Woo et al. [3]. The maximum vertical extent of the turbulence wake is about 1 to 2H for the entire wake for all buildings studied. The turbulence variance excess was approximately constant at a given x/H location from the lowest z/H measured to the height $z/H \approx 1.0$, and the Delta U VAR approaches zero within $z/H \approx 2.0$. Woo et al.'s [3] measurements in neutral flow showed a greater vertical extent of the turbulence wake; hence, the stable approach flow, as might be expected, must inhibit the diffusion of turbulence excess in the wake in the vertical direction. This is because the downward flow along the wake centerline advects less turbulent fluid downward from above.

The maximum Delta U VAR occurring at each x/H is plotted in Fig. 12 for building 3. Similar to the maximum Delta U, this maximum did not occur at the same z/H at each x/H. The figure also shows the neutral flow data from Woo et al. [3] for comparison. The maximum Delta U VAR decays with a power-law exponent of -2.30. The decay rate of Hunt's theory is -2 (Hunt [13]). The slightly higher decay rate seems to originate from the action of the two horseshoe vortices, bringing less turbulent fluid down toward the surface along the wake centerline.

The maximum temperature excess variance Delta T VAR occurring at each x/H on the wake centerline is shown in Fig. 13. The effects of the horseshoe vortices, which did not dramatically alter the results of maximum Delta U VAR, were large for temperature. In the absence of horseshoe vortices, it would be expected that the temperature excess variance would

asymptotically approach zero as a positive value. However, the results show that the maximum Delta T VAR becomes negative before asymptotically approaching zero. The longitudinal vortices, which bring fluid having

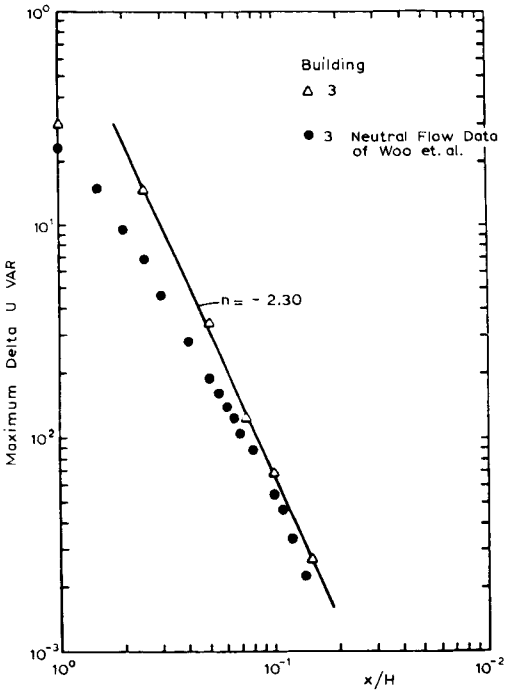

Fig. 12. Comparison of the decay rate of turbulence intensity excess variance behind building 3 with Woo et al. [3].

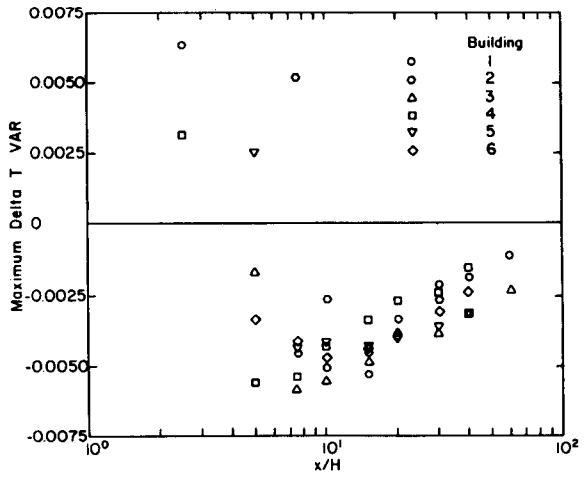

Fig. 13. Decay of temperature excess variance in the wake of buildings.

smaller fluctuation in temperature from the top of the turbulent boundary layer toward the ground on the centerline of the building, result in the negative Delta T VAR. For Delta T VAR the vortex wake is dominant in the near wake compared with the momentum wake effects, and Delta T VAR is still strong at a distance of $x/H = 60$. The long wake of Delta T VAR as compared to the short wake of Delta U VAR, suggests one should use local temperature field characteristics for the evaluation of diffusion of pollutants in the wakes of structures.

6. Conclusions

The effects of a momentum-type wake behind a building in a stably stratified turbulent boundary layer are to decrease mean velocity and mean temperature, but to increase turbulence intensity and temperature-fluctuation intensity. On the other hand, along the centerline of a building wake, horseshoe vortex effects bring higher-momentum, higher-temperature, less-turbulent and smaller-temperature-fluctuation-intensity fluid from higher in the boundary layer, to increase mean velocity and mean temperature and decrease turbulent intensity and temperature-fluctuation intensity near the surface. Thus, in the wake of an isolated building, both momentum and vortex perturbation effects should be taken into consideration.

A theory for temperature distribution in the wakes of buildings was developed considering both momentum and vortex wake effects. With a single free constant, determined from experimental results, the theory predicts the temperature distribution in the far wake of an isolated building. The theory for velocity distribution in the wake of a building considering both momentum and vortex wake effects also showed good agreement with experimental data.

The experimental measurements were compared with the neutral flow data of Woo et al. [3]. The decay rates for the velocity field compared very well in both of these experiments; however, the actual magnitude of the velocity defect was different. The temperature wake extends much farther than the velocity wake, with all the buildings having a temperature wake extending past 60 building heights. The high temperatures and excess velocities observed in the far wake showed that the horseshoe vortices play a very important role in a wake of an isolated building.

Acknowledgment

The work was supported by the Site Safety Research Branch of the U.S. Nuclear Regulatory Commission under contract NRC 04-81-202, Modification 2.

References

1 M.J. Colmer, Some full-scale measurements of the flow in the wake of a hanger, ARC-CP-1166, 1971.
2 W. Frost and A.M. Shahabi, A field study of wind over a simulated block building NASA Rep. CR-2804, 1977.
3 H.G.C. Woo, J.A. Peterka and J.E. Cermak, Wind-tunnel measurements in the wakes of structures, Fluid Dynamics and Diffusion Laboratory Rep. CER75-76 HGCW-JAP-JEC40, Colorado State University, Fort Collins, CO, 1976.
4 J.C.R. Hunt and J.P. Smith, A theory of wakes behind buildings and some provisional experimental results, Central Electricity Research Laboratory Rep. RD/L/N31/69, 1969.
5 J. Counihan, An experimental investigation of the wake behind a two-dimensional block and behind a cube in a simulated boundary layer flow, CERL Lab. Note RD/L/N115/71, 1971.
6 I.P. Castro and A.G. Robins, The effect of a thick incident boundary layer on the flow around a small surface mounted cube, Central Electricity Generating Board Rep. R/M/N795, 1975.
7 R. Lemberg, On the wakes behind bluff bodies in a turbulent boundary layer, University of Western Ontario Rep. BLWT-3.73, 1973.
8 A.C. Hansen, J.A. Peterka and J.E. Cermak, Wind-tunnel measurements in the wake of a simple structure in a simulated atmospheric flow, Fluid Dynamics and Diffusion Laboratory Rep. CER73-74ACH-JAP-JEC43, Colorado State University, Fort Collins, CO, 1975.
9 J.A. Peterka and J.E. Cermak, Turbulence in building wakes, 4th Int. Conf. on Wind Effects on Buildings and Structures, London, 1975, Cambridge University Press, London, 1977.
10 A.C. Hansen and J.E. Cermak, Vortex-containing wakes of surface obstacles, Fluid Dynamics and Diffusion Laboratory Rep. CER75-76ACH-JEC16, Colorado State University, Fort Collins, CO, 1975.
11 J.C.R. Hunt, C.J. Abell, J.A. Peterka and H. Woo, Kinematical studies of the flows around free or surface-mounted obstacles; applying topology to flow visualization, J. Fluid Mech., 86 (1978) 179—200.
12 J. Counihan, J.C.R. Hunt and P.S. Jackson, Wakes behind two-dimensional surface obstacles in turbulent boundary layers, J. Fluid Mech., 64 (1974) 529—563.
13 J.C.R. Hunt, Further aspects of the theory of wakes behind buildings and comparison of theory with experiment, Central Electricity Research Laboratory Rep. RD/L/R/1665, 1971.
14 J.C.R. Hunt, Vortex and momentum wakes behind surface obstacles in turbulent boundary layers, to be published.
15 J.O. Hinze, Turbulence, McGraw-Hill, New York, 1975.
16 S.P.S. Arya, Structure of stably stratified turbulent boundary layer, Fluid Dynamics and Diffusion Laboratory Rep. CER68-69SPSA10, Colorado State University, Fort Collins, CO, 1968.
17 F.B. Smith, The diffusion of smoke from a continuous elevated point-source into a turbulent atmosphere, J. Fluid Mech., 2 (1957) 49—76.
18 K.M. Kothari, Stably stratified building wakes, Ph.D. Dissertation, Colorado State University, Fort Collins, CO, 1979.
19 J.E. Cermak, Applications of fluid mechanics to wind engineering — a Freeman Scholar Lecture, J. Fluids Eng., Trans. ASME, 97 (1975) 9—38.
20 J.E. Cermak and S.P.S. Arya, Problems of atmospheric shear flows and their laboratory simulations, AGARD Conf. Proc., 48 (1970) 12.1—12.16.

21 R.E. Akins, J.A. Peterka and J.E. Cermak, Mean force and moment coefficients for buildings in turbulent boundary layers, J. Ind. Aerodyn., 2 (1977) 195—209.
22 C.C. Alexopoulos and J.F. Keffer, Turbulent wake in a passively stratified field, Phys. Fluids, 14 (1971) 216—224.